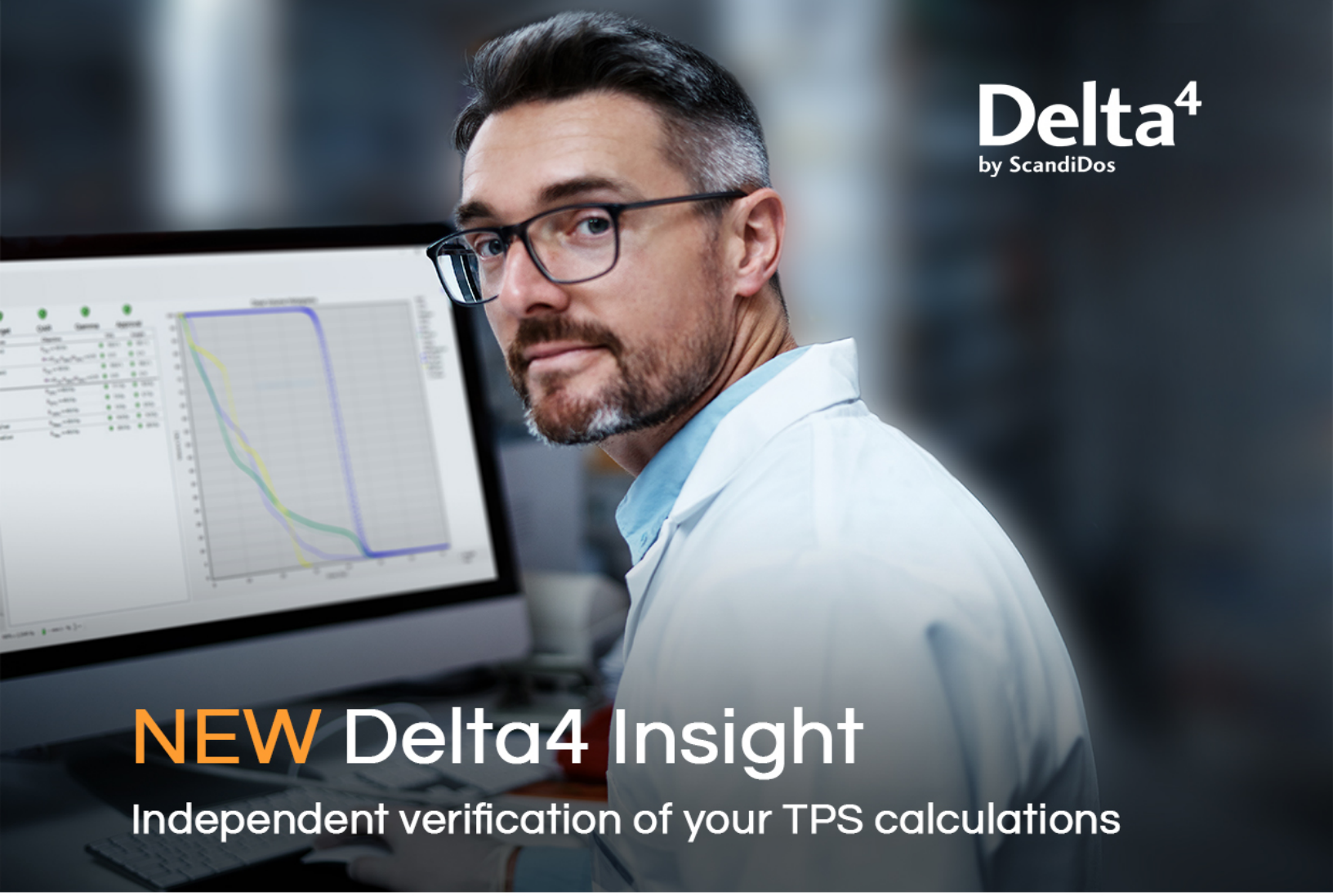

We provide medical physicists with patient QA from prescription to final fraction!

Delta4 Insight is an independent secondary 3D dose calculation software that utilizes a Monte Carlo engine to verify the calculations of a clinic's Treatment Planning System (TPS).

"Our ambition when developing Delta4 Insight was to extend our Delta4 family of products into a full end-to-end verification solution where the customer can be confident that Delta4 provides the true values and not just the deviations."
Görgen Nilsson, CTO, and founder

Delta4 Insight completes the ScandiDos patient QA product portfolio which now covers - patient QA from prescription to final fraction.

Learn more ▶

delta4family.com

Magnetic resonance quantification of the myocardial perfusion reserve with a Fermi function model for constrained deconvolution

Michael Jerosch-Herold,[a] Norbert Wilke, and Arthur E. Stillman
Department of Radiology University of Minnesota Medical School, Minneapolis, Minnesota 55455

Robert F. Wilson
Department of Medicine, University of Minnesota Medical School, Minneapolis, Minnesota 55455

(Received 9 April 1997; accepted for publication 13 October 1997)

The myocardial perfusion reserve, defined as the ratio of hyperemic and basal myocardial blood flow, is a useful indicator of the functional significance of a coronary artery lesion. Rapid magnetic resonance (MR) imaging for the noninvasive detection of a bolus-injected contrast agent as a MR tracer is applied to the measurement of regional tissue perfusion during rest and hyperemia, in patients with microvascular dysfunction. A Fermi function model for the distribution of tracer residence times in the myocardium is used to fit the MR signal curves. The myocardial perfusion reserve is calculated from the impulse response amplitudes for rest and hyperemia. The assumptions of the model are tested with Monte Carlo simulations, using a multiple path, axially distributed mathematical model of blood tissue exchange, which allows for systematic variation of blood flow, vascular volume, and capillary permeability. For a contrast-to-noise ratio of 6:1, and over a range of flows from 0.5 to 4.0 ml/min per g of tissue, the ratio of the impulse response amplitudes for hyperemic and basal flows is linearly proportional to the ratio of model blood flows, if the mean transit time of the input function is shorter than approximately 9 s. The uncertainty in the blood flow reserve estimates grows both at low (<1.0 ml/min/g) and high ($>3-4$ ml/min/g) flows. The predictions of the Monte Carlo simulations agree with the results of MR first pass studies in patients without significant coronary artery lesions and microvascular dysfunction, where the perfusion reserve in the territory of the left anterior descending coronary artery (LAD) correlates linearly with the intracoronary Doppler ultrasound flow reserve in the LAD ($r=0.84$), in agreement with previous PET studies.
[S0094-2405(98)00401-5]

Key words: magnetic resonance, myocardium, blood flow reserve, MR contrast agents

I. INTRODUCTION

It is recognized that the assessment of a coronary artery stenosis should include the measurement of coronary artery flow during maximal vasodilation, and should not be limited to an assessment of resting blood flow. A reduction in resting coronary blood flow is only observed once the stenosis is larger than approximately 80%.[1] The coronary flow reserve (CFR), defined as the ratio of blood flow during maximal vasodilation and basal blood flow, is a useful indicator of the hemodynamic significance of a coronary artery lesion.[1–3] The measurement of the coronary flow reserve in the large epicardial arteries with an intracoronary Doppler ultrasound flow probe is well proven,[4] but not feasible for the determination of the regional blood flow reserve. Measurement of the tissue blood flow reserve or perfusion reserve delineates the spatial extent of a flow impairment in a region of the myocardium subtended by a stenosed coronary artery. In animal studies, the tracer microsphere technique is used for the accurate measurement of myocardial tissue blood flow,[5] but clearly this is not an option for patient studies.

The need for the sensitive, noninvasive detection of myocardial blood flow can be addressed by the external detection of a flow tracer as it distributes in the tissue following its injection. Positron emission tomography (PET) is a gold standard for the noninvasive quantification of absolute myocardial blood flow and the blood flow reserve,[6,7] but its limited availability due to high costs represents a serious handicap. Compared with PET, magnetic resonance (MR) imaging has unique advantages for the noninvasive assessment of myocardial perfusion with an exogenous contrast agent (CA). They are superior temporal and spatial resolution, the absence of any radiation hazards, and the availability of highly stable and inert MR contrast agents of low toxicity. The spatial resolution of 2–3 mm is sufficient to analyze the transmural distribution of blood flow, and better than the spatial in-plane resolution of cardiac PET images.[6]

The quantification of myocardial blood flow with MR has not reached the same acceptance as the PET-based methods. Parameters such as the mean-transit time of the first pass tissue curves provide semiquantitative measures of myocardial blood flow.[8,9] The mean-transit times measured in two first pass experiments, at the baseline, and during maximal vasodilation, cannot readily be compared as the duration of the contrast agent transit through a myocardial region of interest depends on the shape of the arterial input function. Therefore changes in hemodynamic conditions and cardiac output occurring with maximal vasodilation require correcting for differences in the arterial input functions. As a means

to normalize the tissue response to the injection of a contrast agent bolus, we propose to calculate the tissue impulse response by deconvolution of the measured tissue signal time course with the blood pool input function. Deconvolution is inherently a differentiation process and therefore numerically unstable with noise contaminated data. This susceptibility to noise can be reduced by constraining the deconvolution with a parametrized model for the probability distribution of tracer residence times in a region of interest.

The objective of this study was to validate the application to the analysis of MR first pass signal curves of a Fermi function model for the distribution of tracer residence times. We hypothesized that with two MR first pass measurements during rest and hyperemia, the perfusion reserve could be calculated as a ratio of the tissue impulse response amplitudes for hyperemic and basal flow. In a group of patients with varying degrees of microvascular dysfunction we compared the MR perfusion reserve with the coronary flow reserve, measured with an intravascular Doppler ultrasound (US) probe as a gold standard. For patients with a disperse, microvascular flow limitation, which cannot be overcome by collateral supply, the coronary flow reserve and the myocardial perfusion reserve are expected to agree.[7] For simulations, model residue curves were calculated with a physiologically realistic, mathematical model of the myocardial vasculature, and random uniform noise, representative of that observed in MR measurements, was added to these residue curves. We determined the sensitivity of the myocardial blood flow reserve estimates to changes in blood volume, capillary permeability surface area product (PS), and dispersion of the contrast agent bolus upstream of the myocardial region of interest. These simulations establish if under the experimental conditions typically encountered in a MR first pass experiment the ratio of impulse response amplitudes does indeed reflect the ratio of basal and hyperemic blood flows. We analyzed the errors in the estimates of the perfusion reserve for different levels of noise and temporal resolution.

II. METHODS

A. Patient studies

Patients with suspected microvascular disease, also known as ''syndrome X,'' [10] were selected for the MR perfusion studies. Patients with hemodynamically significant lesions on x-ray angiograms were excluded from the MR studies. The MR protocol for the patient studies was approved by the Human Subjects Institutional Review Board of the University of Minnesota Medical School. Written, informed consent was obtained from the patients prior to the MR examination. The CFR was measured prior to the MR examination with an intracoronary Doppler ultrasound catheter probe (NuMed, Hopkinton, NY) and a maximally vasodilating dose of intracoronary adenosine.[11] The technique has been previously described in detail.[12,13] Nitroglycerine (200 μg ic.) was given to assure maximal epicardial coronary dilation. After allowing blood flow velocity to normalize, sequentially greater doses of adenosine (4 μg/m ic. saline, Fujisawa, Inc., Deerfield, IL) were administered as bolus injections. The vasodilator response was assessed as a ratio (peak blood flow velocity divided by basal blood flow velocity) after adenosine bolus. CFR was defined as the maximal vasodilator response, confirmed by no further increase in peak flow with a larger adenosine dose.

MR imaging was carried out within 24 h after cardiac catheterization. Heart rate, systemic blood pressure, and oxygen saturation were monitored during the study with a MR compatible InVivo Omni-Trak recorder (InVivo Research Inc., Orlando, FL). T_1-weighted MR first pass images were acquired during resting conditions, and during maximal hyperemia. To reach maximal vasodilation the intravenous adenosine infusion was started at a rate of 0.05 mg/kg/min and gradually increased to a dosage of 0.14 mg/kg/min, which is sufficient in humans for maximal vasodilation.[11] MR first pass imaging was started after the heart rate had stabilized at the maximal dosage of adenosine.

B. MR multislice first pass perfusion technique

First pass images were acquired at a magnetic field strength of 1.5 T in a whole-body MR system (Siemens Medical Systems, Erlangen, Germany) with a multislice, ultrafast FLASH (fast low angle shot) imaging technique. The heart was imaged in a double-oblique short axis view with the patient in a supine position and breathing freely. The MR signal was T_1 weighted with a saturation-recovery magnetization preparation composed of a nonslice selective 90° radiofrequency pulse, followed by a gradient crusher pulse to dephase the transverse magnetization. It renders the measured signal intensity independent of the heart rate and insensitive to cardiac arrhythmias.[14,15] The magnetization preparation was triggered by the R wave on the electrocardiogram (ECG). The FLASH (fast low angle shot) image acquisition, delayed by 10 ms from the magnetization preparation, had the following parameters: repetition time for each phase-encode step (TR): 2.2 ms; echo time (TE): 1.2 ms; flip angle (α): 18°; slice thickness of 10 mm. The number of phase encoding steps, N, was adjusted to maintain single heartbeat temporal resolution, and fell into a range of 60–90 encoding steps. With a typical matrix size of 128×70, and a rectangular field of view, the in-plane resolution was 2.3 $\times$2.8 mm. Between 40–50 images were acquired for each of 2–3 short axis image planes during 40–50 heartbeats.

Gadopentetate dimeglumine (Gd-DTPA) contrast agent was bolus injected at a rate of 10 ml/s (dosage of 0.025 mmol/kg) through an antecubitally placed catheter whose tip was in the subclavian vein. To obtain baseline MR data, the injection was started with a delay of four to five heartbeats after beginning the acquisition of images. The T_1 weighting from the saturation recovery magnetization preparation in the FLASH sequence results in a linear relationship between the signal intensity and $1/T_1$ over a limited range of CA concentrations. The saturation-recovery prepared FLASH signal was measured in a series of titrated solutions of Gd-DTPA with concentrations from 0 to 5.3 mmol/L of Gd-DTPA. The T_1-Turbo-FLASH signal obtained with a flip angle of α

$=18°$ was an excellent measure of CA concentration over a range of 0–0.7 mmol/l, and underestimated the CA concentration by -4% at 1 mmol/L, -11% at 2 mmol/L, and -26% at 3 mmol/L.

C. Image analysis

All images were transferred from the MR scanner to a computer workstation (Sun Microsystems, Mountain View, CA) and evaluated with a custom written image analysis program. Seven circular regions of interest (ROI) were manually placed to cover the anterior, midseptal, posterior, posterior papillary muscle, lateral, anterior papillary muscle sections of the myocardium, and a central portion of the blood pool in the left ventricular cavity. Due to the relatively slow breathing motion during acquisition of 40–50 images per image plane, the position of the heart shifted in the field of view. To correct for this predominantly translational motion of the heart, the position of the ROIs was checked, and if necessary, adjusted in each image frame by reference to landmarks such as the papillary muscles. Signal time courses were obtained by spatially averaging the image intensity values over the ROIs. For all experimental data, including the measured input curves used for simulations, the mean value of the baseline signal before the appearance of the contrast agent in the LV blood pool was subtracted from all signal versus time curves. The signal curves were scaled to correct for spatial inhomogeneities in the sensitivity profile of the receiver radiofrequency coil.

D. Deconvolution fit of tissue signal curves

With the MR first pass technique one detects indirectly the quantity of a contrast agent, $q(t)$, in a tissue ROI. From the principle of mass balance it follows that the amount of tracer in the ROI at any time, $q(t)$, is simply the difference between the amount of tracer that was washed in and washed out.[16] If we denote the inflow and outflow tracer concentrations by $c_{\text{in}}(t)$ and $c_{\text{out}}(t)$, this can be written as

$$q(t)=F\int_0^t[c_{\text{in}}(s)-c_{\text{out}}(s)]\cdot ds. \tag{1}$$

F is the rate of flow. For a linear and stationary system the inflow and outflow tracer concentrations, $c_{\text{in}}(t)$ and $c_{\text{out}}(t)$, are related through convolution of $c_{\text{in}}(t)$ with the transfer function, $h(t)$:[17]

$$c_{\text{out}}(t)=\int_0^t c_{\text{in}}(s)\cdot h(s-t)\cdot ds=c_{\text{in}}(t)\otimes h(t). \tag{2}$$

The transfer function, $h(t)$, gives the probability that with an idealized instantaneous input (a Dirac delta function) at $t=0$, a tracer molecule has left the ROI at time t. This means that $h(t=0)=0$, as a tracer molecule cannot instantaneously traverse a ROI. Equation (1) can be rewritten as

$$q(t)=F\int_0^t c_{\text{in}}(s)\otimes[1-h(s)]\cdot ds=R_F(t)\otimes c_{\text{in}}(t), \tag{3}$$

where we defined the flow-weighted impulse response $R_F(t)$ as

$$R_F(t)=F\cdot\left[1-\int_0^t h(s)ds\right]=F\cdot R(t). \tag{4}$$

$R(t)$ represents the probability that a tracer molecule remains in the ROI up to time t. We note here that as $h(t=0)=0$, the initial amplitude of the impulse response, $R_F(t=0)$, equals F, the rate of flow.[16] With the washout of the contrast agent, $R_F(t)$ decays with time from its initial amplitude F at $t=0$, as the probability that a tracer molecule remains in the ROI decreases.

The analysis of the MR signal versus time curves is based on the following assumptions and experimental conditions.

(1) The MR image intensity is linearly proportional to the regional CA concentration for the CA dosage used in this study (0.025 mmol/kg of Gd-DTPA). This linear relationship is independent of the heart rate with a saturation recovery prepared gradient echo signal.[14,15]
(2) The relationship between image intensity and CA concentration is the same in both the blood pool and the myocardium.[18,19]
(3) In the myocardium the linearity assumption holds with a short TR gradient echo sequence with a relatively high flip angle that minimizes the effects of water exchange, and a no-exchange model can be applied.[20]
(4) The signal time course in the LV blood pool can be used as an input function, $c_{\text{in}}(t)$, for deconvolution of the tissue curves, as previously validated in PET studies.[21]
(5) The shape of the tissue impulse response, $R(t)$, can be approximated with a Fermi function.[22]

A Fermi function model was previously applied to deconvolve first pass curves obtained with dynamic computed x-ray tomography.[22] The analytical expression for the Fermi function model is

$$R_F(\tau)=F\cdot\left[1-\int_0^t h(s)ds\right]=F\cdot\left[\frac{1}{\exp[(\tau-\tau_0-\tau_d)\cdot k]+1}\right]\cdot\theta(t-\tau_d). \tag{5}$$

$\theta(t-\tau_d)$, a unit step function, equals 0 for $t<\tau_d$ and 1 for $t>\tau_d$. It accounts for the delay τ_d (adjusted in time increments equal to the RR interval) between the LV signal time course used for $c_{\text{in}}(t)$ and the input to the region of interest being analyzed. A shortcoming of most tomographic imaging methods is the inability to measure the concentration at the entrance to the ROI, in part because the ROI does not have a single, or a well-defined vascular input. τ_0 characterizes the width of the shoulder of the Fermi function, during which little or no contrast agent has left the ROI, and k is the decay rate of $R_F(t)$ due to contrast agent washout.

The initial 30–40 s long signal record of the first pass signal versus time curves for tissue ROIs were fit to the Fermi function model with a Marquardt–Levenberg nonlinear least squares fitting algorithm,[23] by letting the parameters

F, τ_0, and k vary and maintaining τ_d fixed, at a user determined value. Both $c_{in}(t)$ and $R_F(t)$ were zero filled to 256 points. Based on the convolution theorem, the fitting function $q(t)$ was calculated from $c_{in}(t)$ and $R_F(t)$ by multiplying their Fourier transforms. The best fit parameter values were observed to be ''unique'' (i.e., identifiable) and independent of the choice of starting values. The MR regional myocardial perfusion reserve was calculated as a ratio of the $R_F(t=0)$ amplitudes for basal and hyperemic flow. It is this ratio that was compared to the intracoronary Doppler US flow reserve in the patient studies, and to the ratio of model blood flows in the simulations.

E. Modeling residue functions and sensitivity analysis

Simulations were carried out to determine how vascular volume, capillary permeability, and upstream dispersion, influence the flow reserve estimate, as these quantities do not explicitly enter the Fermi function model of Eq. (5). Residue curves were calculated with a physiologically realistic, axially distributed model of blood tissue exchange with multiple parallel flow pathways.[17] The computer code for the MMID4 model is available from the National Simulation Resource (Bioengineering, University of Washington, Seattle). This mathematical model of the vascular system accounts in detail for vascular flow and dispersion, arterial, arteriolar, and capillary volumes, interstitial volume, and capillary permeability. The model, referred to as Multiple indicator, Multiple path, Indicator Dilution 4 region model (MMID4), has previously been described in detail.[17,24] Briefly, a large conduit vessel outside the model region of interest accounts for dispersion and delay upstream of the myocardial region of interest. All the flow entering the region of interest passes through this large conduit vessel. Within the myocardial region of interest there are N parallel flow pathways. Each pathway is composed of a small vessel in series with an axially distributed capillary blood–tissue exchange unit.[17] Vascular operators are used to model indicator dispersion and delay in the large conduit vessel, upstream from the region of interest, and in arteries and arterioles within the region. The vascular operators are dispersive delay lines, having a relative dispersion, RD, defined as the standard deviation divided by the mean-transit time (MTT).

The effects of regional flow heterogeneity are modeled by apportioning flow among the multiple pathways according to a slightly right skewed lagged normal density distribution. The total quantity of indicator in the model region of interest corresponds to the residue curve and encompasses the small vessels and the capillary–tissue units, but does not include the large vessel upstream from the region of interest. The capillaries are modeled as axially distributed blood–tissue exchange units, in which the capillary permeability (PS) was varied to study the effects of contrast agent leakage from the capillary bed into the interstitial space.

Parameters for the MMID4 model were set to values validated in multiple indicator dilution experiments with normal canine hearts.[25] The model capillary volume (V_p) was 0.04 ml/g for basal flow, and 0.09 ml/g for hyperemic flow ($F \geqslant 1.5$ ml/min/g), unless stated otherwise. The large vessel arterial (V_{art}) and arteriolar (V_{artl}) volumes were 0.02 and 0.03 ml/g, respectively, and the volume of the upstream conduit vessel (V_{tube}) was 0.05 ml/g. The large vessel volumes were kept constant. It has been established that the large vessel volume is not significantly different during hyperemia and rest.[26] A blood flow of 1.0 ml/min/g was assumed as a reference for resting conditions. The relative dispersion (RD) was set to 0.48 for the upstream conduit vessel, arteries, and arterioles. These parameter choices were used as default values for all simulations, unless otherwise stated. For one representative tissue curve, obtained in the same patient as the input functions discussed above, we optimized the MMID4 model parameters for flow (F) and the capillary plasma volume (V_p) with a nonlinear least-squares algorithm based on sensitivity functions. The parameter starting values used for the optimization were $F=1.0$ ml/min/g and $V_p=0.04$ ml/g.

The modeling results presented here make use of two blood pool input functions measured in the same patient under resting conditions, and during hyperemia. The signal versus time curve measured during adenosine induced hyperemia (RD=0.33 and MTT=4 s) in the LV blood pool was chosen for simulations with model blood flows at or above 1.5 ml/min/g, while the LV input function for resting conditions (RD=0.44 and MTT=7 s) was used for model residue curves calculated for flows less than 1.5 ml/min/g.

F. Monte Carlo simulations

Monte Carlo simulations were carried out to evaluate the confidence in the parameter estimates obtained by least-squares fitting of the Fermi function model to the MMID4 model residue curves. Uniform distributions of random numbers falling within a range of 0–1.0 were generated with a linear congruential generator with a period of 2.1×10^9, and then scaled to a noise level that was judged representative of that observed in the MRI data. We generated for a simulated model residue curve, 128 residue curves, identical to each other, except for the added noise. The Fermi function model was fit with a nonlinear least-squares Levenberg–Marquardt algorithm to each noise contaminated model residue curve. Both the mean and the standard deviation of the distribution of the $R_F(t=0)$ values from 128 trials for each calculated model residue curve were determined. The tissue perfusion reserve (PR) was calculated as ratio of the flow estimates for ''hyperemia''—model blood flows $F \geqslant 1.5$ ml/min/g—and a reference ''rest'' state with a flow $F=1.0$ ml/min/g. The maximum error of the flow reserve estimate (ΔPR) was calculated from the mean values of $R_F(t=0)$ for rest and hyperemia, F_r and F_h, respectively, and their standard deviations, σ_r and σ_h, respectively, as

$$\Delta \mathrm{PR} = \sqrt{\left(\frac{\sigma_h}{F_r}\right)^2 + \left(\frac{F_h \cdot \sigma_r}{F_r^2}\right)^2}. \tag{6}$$

Monte Carlo simulations were carried out with the above listed default parameters, except that some model parameters were varied over a physiologically realistic range. Model

blood flows covered a range from 0.5 to 4.0 ml/min/g, the capillary permeability surface area product was changed from 0.25 to 8 ml/min/g, and the capillary plasma volume was increased from 0.04 to 0.09 ml/g.

Establishing the effects of noise on the flow reserve estimates requires a measure of the noise observed in an MR first pass experiment. The signal-to-noise ratio of the baseline signal before contrast enhancement can be arbitrarily varied by changing the delay between magnetization preparation and FLASH image acquisition. The level of noise in the MR signal curves was therefore judged by the contrast-to-noise ratio (C/N), defined as the peak signal after subtraction of the baseline signal, divided by the standard deviation of the baseline signal. The C/N values quoted for the simulations refer to the peak signal of a model residue curve calculated with the default modeling parameters. The Monte Carlo simulations were carried out for a C/N of 6:1, except when stated otherwise. This C/N is representative of that observed in the MR first pass studies in patients under resting conditions.

Finally, to assess the consequences of a more disperse injection of contrast agent than encountered in the patient studies, we calculated a series of model residue curves with gamma-variate pseudoinput functions with MTTs of 9 s and 16 s, respectively. A gamma-variate function is commonly used to fit first pass CA time curves,[27] and was applied here to model the CA concentration time course:

$$c(t) = C \cdot t^{\nu} \cdot \exp(-t/u). \tag{7}$$

The mean-transit time (MTT) is given by $\mathrm{MTT} = (\nu + 1) \cdot u$.

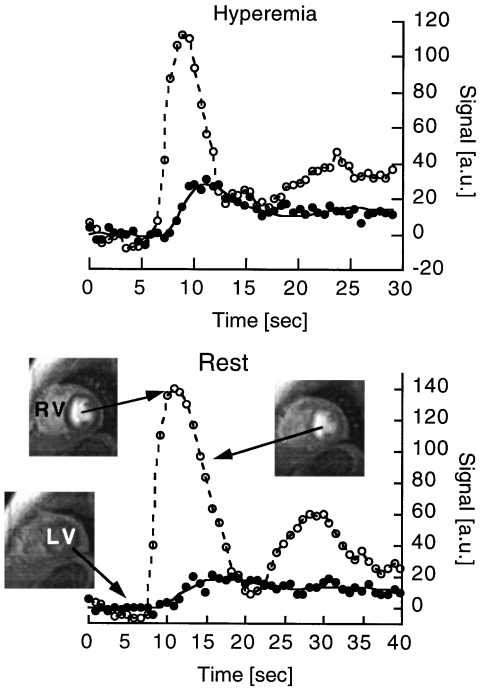

FIG. 1. Turbo-FLASH signal time courses for regions of interest in the LV blood pool (open circles connected with a dotted line) and the anterior wall segment (solid circles), during rest (lower graph) and maximal hyperemia (upper graph). The three images in the graph for the rest study show the same double oblique short axis view of the heart at the level of the papillary muscles. The arrows assign these images, depicting transit of the contrast agent through the LV blood pool, to the corresponding points on the signal intensity curve for the LV blood pool. The solid lines through the measured signal time course for the anterior wall segment represent the least-squares fits obtained with a Fermi function model for the tissue impulse response.

III. RESULTS

A. Perfusion reserve in patients with microvascular disease

Figure 1 shows signal versus time curves in one patient for regions of interest in the blood pool of the left ventricular cavity, and the anterior wall segment, under basal and hyperemic conditions. In this patient the perfusion reserve in the LAD territory averaged 3.03 ± 0.7. The LV input function for resting conditions had a relative dispersion of $\mathrm{RD} = 0.44$ and a MTT of 6 s. The signal versus time curve measured during adenosine-induced hyperemia had a relative dispersion of $\mathrm{RD} = 0.33$ and a MTT of 4 s. A total of nine patients underwent both the MR perfusion reserve measurement and in the catheterization laboratory the intracoronary Doppler US flow reserve measurement. The Doppler US CFR in the LAD, averaged 2.38 ± 0.59 ($N = 9$) vs 2.14 ± 0.57 ($N = 9$) for the MR myocardial perfusion reserve in the LAD territory. A two-tailed paired t test showed that the means for the CFR (Doppler US) and the MR myocardial perfusion reserve were not significantly different ($p > 0.8$). A comparison of the MR myocardial perfusion reserve in the territory of the LAD with the LAD CFR is shown in Fig. 2. The vertical error bars show the standard deviations for the MR perfusion reserve in the territory of the LAD. The horizontal error bars for the Doppler US coronary flow reserve were calculated as 4% of the measured value, which is the interstudy variability for the intracoronary Doppler US measurement in our laboratory.[4] For this study the CFR measurement error was therefore estimated to be 4% of the measured value. Linear regression analysis yields a slope of 0.98 ± 0.24 (best fit value $\pm$ standard error), an intercept value of 0.00 ± 0.57, and a regression coefficient of $r = 0.84$. The perfusion reserve in the territory

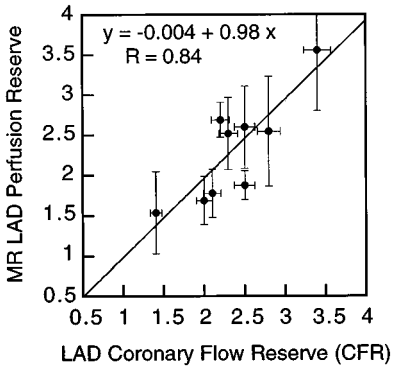

FIG. 2. Comparison of the coronary flow reserve measured with an intravascular Doppler ultrasound probe in the LAD and the MR perfusion reserve in the territory of the LAD. The vertical error bars show the standard deviations for the MR perfusion reserve. The horizontal error bars for the Doppler US coronary flow reserve were calculated as 4% of the measured value, which is interstudy variability for this measurement.

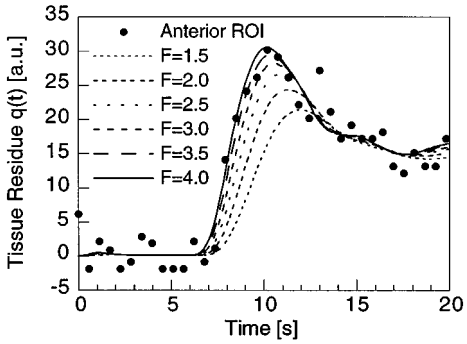

FIG. 3. Model tissue residue curves calculated for different blood flows from 1.5 to 4.0 ml/min/g, using a LV input function measured with MR imaging in a patient during maximal vasodilation. To illustrate the fact that the model does realistically reproduce the measured tissue residue curves, the figure also includes the signal time course observed in the same patient during hyperemia in the anterior wall segment.

of the LAD, and the perfusion reserve averaged over all myocardial segments, were not significantly different ($p = 0.95$).

B. Modeling results

Calculated model residue curves obtained with the MMID4 model are shown in Fig. 3 for flows in the range from 1.5 to 4.0 ml/min/g. To illustrate the similarity between simulated and measured residue curves, Fig. 3 shows a representative tissue curve for the anterior wall segment obtained in the same measurement as the LV input curve in Fig. 1. The model curves suggest that blood flow in the anterior wall segment was in the neighborhood of 3–4 ml/min/g. This was confirmed by optimizing the MMID4 model parameters for flow and capillary volume. The best fit values for flow and capillary volume were $F = 3.85$ ml/min/g and $V_p = 0.09$ ml/g.

Noise contaminated model residue curves for ''rest'' (model blood flow $F = 1.0$ ml/min/g) and ''hyperemia'' ($F = 1.5$, 2.0, 2.5, 3.0, 3.5, 4.0 ml/min/g) were fit to the Fermi model of $R_F(t)$ in Eqs. (3)–(5) to estimate the tissue blood flow reserve. An example of such a fit to a noise contaminated model tissue curve for $F = 4.0$ ml/min/g and a C/N of 6 is shown in Fig. 4. Flow estimates obtained from the ratio of the impulse response amplitudes for ''rest'' and ''hyperemia'' are plotted in Fig. 5 versus the ratio of model blood flows. A linear correlation with a slope of 1.04 ± 0.029 was observed between the estimated flow reserve and the model blood flow ratios (Pearson correlation coefficient $r = 0.98$).

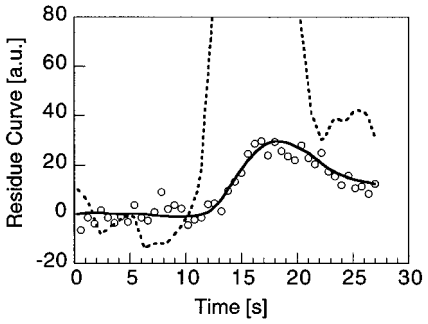

FIG. 4. The fit (solid line) was obtained by least-squares fitting the Fermi model for constrained deconvolution to a model residue curve, to which uniform, random noise had been added (open circles). The parameters for calculation of the model residue curve were $V_p = 0.09$ ml/g; $F = 4$ ml/min/g; PS = 1.0 ml/min/g; number of paths = 10; number of segments = 10; $V_{tube} = 0.05$; $RD_{tube} = 0.48$; $V_{artery} = 0.02$ ml/g; $RD_{artery} = 0.48$; $V_{artl} = 0.03$; $RD_{artl} = 0.48$. The dotted line shows part of the input function measured in a patient during hyperemia and used for calculation of the model residue curve (see also Fig. 1; hyperemia).

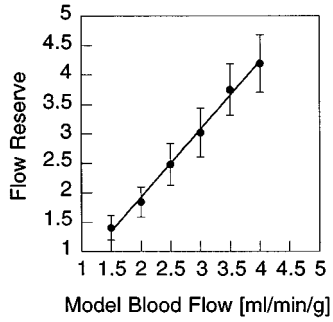

FIG. 5. Perfusion reserve calculated from the ratio of the impulse response amplitudes, $R_F(t=0)$, for each of the model residue curves shown in Fig. 3 above, and $R_F(t=0)$ for a reference ''rest'' state with a blood flow of $F = 1.0$ ml/min/g. The error bars show the maximum error calculated from the standard deviations of $R_F(t=0)$ for rest and stress.

Variation of the dispersion in the large conduit vessels upstream from the model ROI did result only in minor changes in the calculated residue curves. An example for RD = 0.08 and RD = 0.48 is shown in Fig. 6. After adding noise to the calculated model residue curves the flow estimates obtained from Eqs. (5)–(7) were not significantly different for a C/N = 6.

The capillary permeability surface area product (PS) was varied over a range from 0.25 to 8 ml/min/g, to determine the changes in the perfusion reserve estimate resulting from increased leakage of Gd-DTPA into the interstitial space. Changes in the shape of the model residue curves resulting from a change in PS were most pronounced at high flows. Figure 7 shows a set of model residue curves for PS values of 0.25, 0.5, 1.0, 2.0, 4.0, and 8.0 ml/min/g and a blood flow of $F = 4.0$ ml/min/g. The perfusion reserve was determined

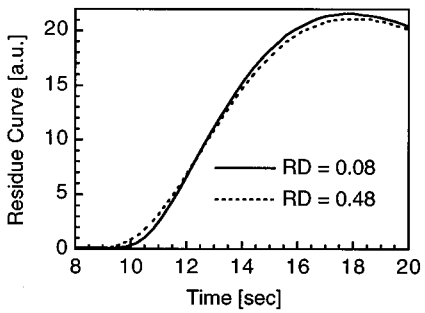

FIG. 6. Model tissue residue curve for two different values of the relative dispersion (RD), in the conduit vessel upstream from the model region of interest. The relative dispersion is defined as the standard deviation divided by the mean transit time.

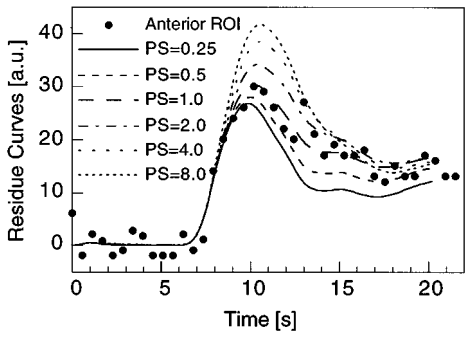

FIG. 7. Model tissue residue curves calculated with MMID4 for a flow of 4.0 ml/min/g and for different capillary permeability surface area products (PS=0.25, 0.5, 1.0, 2.0, 4.0, and 8.0 in units of ml/min/g), using a LV input function measured in a patient during maximal vasodilation. The peak intensity increases monotonically with PS. A measured signal time course (solid circles) for the anterior wall segment, obtained in the same patient as the LV input curves, is shown for comparison.

from these model residue curves, using a model residue curve with PS=1.0 ml/min/g and $F=1.0$ ml/min/g as reference for the ''rest'' state. The estimate of the perfusion reserve deviates by less than 10% from the ratio of model flows (1:4) over this range of PS values. It increases slightly with increasing PS values, and a linear fit results in a slope of 0.027 ($R=0.45$).

The capillary volume (V_p) was varied over a range from 0.04 to 0.12 ml/min/g. Figure 8 shows the flow reserve estimates for this range of values of capillary volume and flows of 1.5 ml/min/g and 4.0 ml/min/g. A model residue curve for a blood flow of 1.0 ml/min/g and a capillary blood volume of 0.04 ml/g was used as a reference curve for the resting state in the determination of the flow reserve.

For blood flows in the range from 0.5 to 1.0 ml/min/g we found that the error in the ratio of flow estimates increases for flows in the lower part of this range. A model residue curve for a model blood flow of 1.0 ml/min/g was again used as reference. All model residue curves used for these simulations covering flows from 0.5 to 1.0 ml/min/g are based on the input function measured in a ''resting'' state. Monte Carlo simulations were run for contrast-to-noise (C/N) ratios of 6, and, in addition, for C/N=12. Figure 9 shows that the standard deviation of $R_F(t=0)$ at a flow of 0.5 ml/min/g is approximately seven-fold higher for a C/N=6 than for C/N =12.

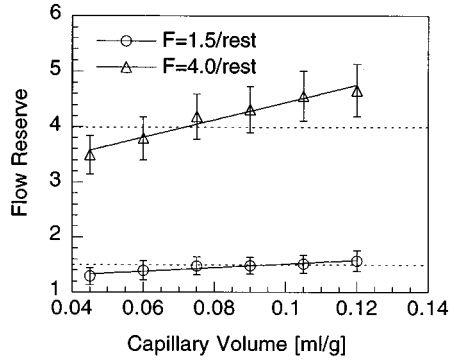

FIG. 8. Model residue curves with random uniform noise added were calculated for several capillary volumes (0.04–0.12 ml/g) and for a blood flow of $F=4.0$ ml/min/g to represent the ''hyperemic'' state. The figure shows the variation of the perfusion reserve, calculated as the ratio of the initial impulse response amplitude for ''rest'' and ''hyperemia,'' versus the model capillary volume. A model residue curve with $F=1.0$ and $v_p=0.04$ ml/g was used to represent the ''rest'' state. The error bars show the maximum error calculated from the standard deviations of $R_F(t=0)$ in 128 trials.

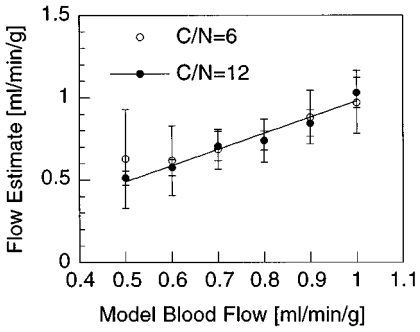

FIG. 9. Variation of the flow estimate at low flows from 0.5–1.0 ml/min/g. The error bars show the maximum error calculated from the standard deviations of $R_F(t=0)$ for ''rest'' and ''stress.''

Reducing the temporal resolution of the model residue curves, while leaving all model parameters unchanged, increased the error of the flow reserve estimates. We repeated the simulations summarized in Figs. 3 and 5 and reduced the sampling rate by a factor of 2 and 3, respectively. This directly corresponds to first pass measurements where images are acquired every second and every third heartbeat, respectively. Figure 10 shows the variation of the flow reserve with flows from 1.5 to 4.0 ml/min/g and sampling rates of 1, 0.5, and 0.3 images/heartbeat. The sampling rate for the model residue curve for the ''resting'' state ($F=1.0$ ml/min/g) was kept constant, as sampling rates of less than one image/heartbeat are most likely to occur with elevated heart rates during hyperemia.

Increased dispersion of the input function compromises the quantification of the flow reserve. Model residue curves were calculated for two gamma-variate input functions with

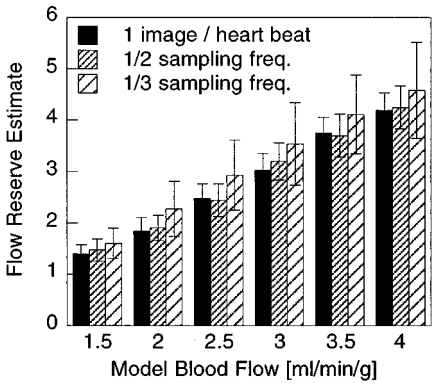

FIG. 10. Variation of flow reserve with model blood flow for three residue curve sampling rates of 1.0, 0.5, and 0.3 samples/heartbeat (from bottom to top) and a contrast-to-noise ratio of 6:1. The error bars show the maximum error calculated from the standard deviations of $R_F(t=0)$ for ''rest'' and ''stress.''

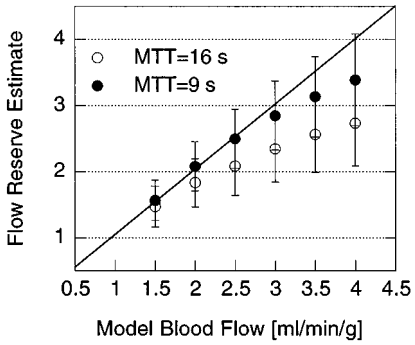

FIG. 11. Model residue curves for flows in the range from 1.0 to 4.0 ml/min/g were calculated for two input functions with mean-transit times of 9 and 16 s, respectively. The model residue curve for $F=1.0$ ml/g/min was used as a reference residue curve for the ''rest'' state. The graph shows the variation of the blood flow reserve for the two input functions. The errors in the estimates of the MR flow reserve are largest with the most disperse input function.

MTTs of 9 and 16 s, respectively. A MTT of 16 s probably represents a reasonable scenario for the slow peripheral administration of contrast agent. The model residue curves were not as spread apart in the vertical direction as is seen with a more rapid bolus input function (e.g., Fig. 3). For the input function with MTT=16 s, Fig. 11 shows that at flows of 3.0 ml/g/min and higher, the flow reserve estimates deviate significantly (>one standard deviation) from the identity relationship. For MTT=9 s, the differences between the flow reserve estimate and the line of identity are not significant up to flows of 4.0 ml/min/g.

IV. DISCUSSION

We have demonstrated how the model-constrained deconvolution of residue curves, sampled with rapid MR imaging under resting and hyperemic conditions, provides a means for the robust and noninvasive estimation of the myocardial perfusion reserve. The MR contrast agents in most common use do not cause hemodynamic changes,[28] and therefore justify the assumption of a stationary residue response. Previous attempts to estimate myocardial blood flow with MR first pass imaging and extracellular contrast agents were in most cases based on the central volume principle.[8,9] The application of the central volume principle to the measured signal curves assumes that all contrast agents reside in the ROI, at least during the acquisition of one image in the first pass,[29] and this is only likely to occur with a central bolus injection of the MR contrast agent. The deconvolution of the tissue signal curves circumvents this major limitation to the application of the central volume principle. The determination of the residue impulse response amplitude is necessary for a comparison of tissue signal curves acquired with two separate bolus injections under hemodynamically distinct conditions. The Fermi function model for the constrained deconvolution can, in principle, can be applied to any shape of input and tissue signal curve, and is not limited to cases where signal curves are well approximated by gamma-variate functions. Separation of the signal components from the first pass and recirculation is not necessary. In many MR patient studies, the contrast agent bolus, once it reaches a tissue region of interest, will be sufficiently disperse to make the distinction between the first pass and recirculation difficult, or impossible. This is a well-known problem for fitting tissue signal curves to a gamma-variate function, where the recirculation component should be excluded from the gamma-variate fit for the correct estimation of the tissue mean transit time. The simulations show that the quantification of the perfusion reserve requires a sufficiently rapid MR imaging technique, in particular, during hyperemia, to capture the first pass of the contrast agent with a temporal resolution of approximately one image per heartbeat in each image plane. This is now feasible on clinical scanners with short gradient rise times.

A. Patient studies

The patient studies demonstrate that in the absence of significant coronary lesions the myocardial perfusion reserve, determined noninvasively with the MR first pass technique, correlates with the CFR. We focused on the human studies on patients with suspected microvascular dysfunction resulting in a diffuse flow limitation at the microvascular level that cannot be compensated by collateral flow. For this special case one expects, based on the principle of mass balance, that the myocardial perfusion reserve correlates linearly with the CFR. By contrast, the CFR in an artery with a hemodynamically significant lesion does not predict the level of ischemia in the myocardium subtended by the stenosed coronary artery, as collateral vessels can compensate for the flow limitation. In patients with coronary artery disease, the measurement of the myocardial perfusion reserve would allow the regional assessment of the functional significance of a coronary artery lesion. Nevertheless, for the sake of validating the proposed MR methods, we selected patients without a hemodynamically significant coronary artery lesion, but instead with different degrees of microvascular flow impairment, so that no discrepancy is to be expected between the coronary flow reserve and the myocardial flow reserve. Previous PET studies demonstrated that one should indeed observe a linear correlation between the coronary flow reserve and the myocardial perfusion reserve for such a microvascular flow limitation.[7] PET is currently considered the gold standard for the noninvasive quantification of myocardial blood flow. The linear correlation observed in this study ($r=0.84$) compares favorably with that observed in previous PET studies in ''syndrome X'' patients.[7]

For comparison with the MR perfusion reserve, the coronary flow reserve was measured in the LAD in patients with microvascular dysfunction. Measurement of the CFR is generally an invasive procedure. The gold standard for quantification of the CFR is based on the measurement during catheterization of the red blood cell flow velocity with intravascular Doppler US.[4,12,13] The noninvasive quantification of the CFR in the left anterior descending coronary artery with cine MR imaging has recently been demonstrated[30,31] but has not replaced the more invasive

Doppler US procedure, which is still considered a gold standard.

An important aspect of any MR imaging technique applied to the quantitative assessment of myocardial perfusion is the relation between the measured signal and the CA concentration. It has been shown that $1/T_1$ follows the same linear relationship with respect to CA concentration in both blood and soft tissues.[18] With a saturation recovery prepared gradient echo sequence,[14,15] as used in this study for T_1 weighting, the relation between the measured signal intensity and the contrast agent concentration is independent of the heart rate. Calibration experiments on Gd-DTPA saline phantoms with the saturation recovery prepared FLASH sequence showed that over a range of contrast agent concentrations from 0 to 2 mmol/L, a linear signal response model results at worst in an underestimate of 11% with respect to the true shape of the input function. The peak concentration of contrast agent in the LV can be estimated by assuming for a 80 kg, 32–58 yr old male a cardiac output of 7 L/min.[32] The Stewart–Hamilton principle of indicator dilution[33] relates the cardiac output ($\dot{Q}$), and the amount injected indicator (I) with the measured time course of indicator concentration $c(t)$ by

$$\dot{Q} = \frac{I}{\int_0^\infty c(t) \cdot dt} = \frac{I}{c_{\text{av}} \cdot t_d}, \tag{8}$$

where t_d is the duration of the first pass in the LV blood pool and c_{av} is the average contrast agent concentration. In the patient studies an injection dose of 0.025 mmol/kg of Gd-DTPA (80 kg body weight) was used. Typically with an injection into an antecubital vein the MTT of the first pass is on the order of 5–6 s, and passage through the left ventricle lasts for approximately 10 s at a heart rate of 75 beats per minute. Assuming that during pulmonary passage 20% of the contrast agent is extracted, the mean indicator concentration in the left ventricle is approximately 1.4 mmol/L. By fitting the first pass curves for the LV blood pool to a gamma-variate function we find that with a mean indicator concentration of 1.4 mmol/L, the peak concentration will be on the order of 1.8 mmol/L. At this peak concentration the saturation of the signal peak is -11%, and less at lower CA concentrations. This justifies as a first approximation the use of a linear approximation for the relation between tracer concentration and signal response.

The signal from a pixel in a tissue region is a weighted average of the contributions from the vascular compartment and the interstitial space, which may have different CA concentrations during the wash-in of CA. The weighting factors of this average involve the compartmental volumes that are not known *a priori*, and, in addition, a CA extraction fraction varies with flow.[34] It is therefore practically impossible to correct for saturation of the signal in a tissue ROI at high contrast agent concentrations. The additional dispersion occurring between the site in the LV where the input function was sampled, and the coronary resistance vessels virtually assures that the peak concentration of the contrast agent is lower in capillaries, and arterioles, than in the LV blood pool, although it remains uncertain how much lower. The most practical way to circumvent the uncertainties about signal saturation in tissue ROIs is to use a low contrast agent dosage such that the signal saturation in the LV blood pool is within acceptable limits. Saturation of the signal in the blood pool during transit of the contrast agent does not alter the findings from the simulations, which used the signal curves for ROIs in the LV as input functions. It simply means that the signal versus time curves measured in the blood pool are not an exact measure of contrast agent concentration, but this discrepancy due to saturation was less than 10%–15%.

B. Simulations

The effects of varying the myocardial blood flow, the capillary permeability, the capillary volume, and the dispersion upstream from the myocardial region of interest, were studied in simulations with the MMID4 model to determine the effects of these changes on the estimate of the blood flow reserve. It is practically impossible to control these parameters in a physiological model. We resorted to the use of a well-validated, multipathway and axially distributed model of myocardial blood flow for the simulations. The advantages of a distributed model, such as the MMID4 model, for calculating residue curves have been discussed in detail before.[24,29]

The Fermi function model for constrained deconvolution used in this study does not account for the dispersion occurring between the sampling site for the input function and the region of interest. The dispersion of the contrast agent bolus in the upstream conduit vessels is less than in the coronary resistance vessels where flow is heterogeneous,[35] and the simulations show therefore not unexpectedly that the effects of varying the upstream dispersion do not significantly alter the shape of the residue curves for an extracellular MR contrast agent. For the experiments and the simulations it was observed that a time delay between the LV signal versus the time curve and the tissue residue curve can be accounted for by time shifting the residue impulse response.

Errors in the flow reserve estimates increase at low (<1.0 ml/min/g) and high flows (3–4 ml/min/g). The errors at low flows can be traced to the decrease of the signal peak-enhancement occurring with a reduction in flow. This translates into a reduced contrast-to-noise ratio for low flows. The error in the flow reserve estimate for high flows is mostly due to the decreased separation of residue curves as the model blood flow is incremented in equal steps in the high flow range (see Fig. 3). The relatively large error in the flow reserve estimate at low and high flows is not attributable to the modeling analysis but inherent to the measurement technique. These errors could become smaller if the input function dispersion is reduced, and if the temporal resolution is increased to better discriminate flow changes in the high flow range.[24]

While the flux across the capillary membrane might, in principle, contribute to the flow rate estimate obtained with the Fermi model, the variation of PS does not significantly change the flow reserve estimate, based on the early phase of

contrast agent wash-in. The variation of PS alters the kinetics of the distribution between vascular and interstitial space, but does not significantly affect the rate at which the contrast agent is washed into the tissue region of interest following a rapid bolus injection. The simulation results in Fig. 8 illustrated that both the peak concentration and the rate at which the CA concentration returns to its baseline value after the contrast agent bolus injection are markedly altered with changes in PS. It was previously observed in indicator dilution experiments that the capillary PS in the myocardium is proportional to myocardial blood flow.[36] To account for this observation the permeability surface area product PS was varied in the simulations over a range from 0.5 to 8 ml/min/g for model residue curves corresponding to blood flows in the range from 1.5–4.0 ml/min/g. The PS value was kept constant at 1.0 ml/min/g for the reference model residue curve representative of the rest state. While the capillary permeability to Gd-DTPA is not exactly known, we found through the simulations that even at a relatively high value for PS of 8 ml/min/g the change in the mean of the blood flow reserve estimate is significantly less than the error from measurement noise.

Changes in the capillary volume occurring with vasodilation cause a larger variation in the flow reserve estimate than changes in PS. The capillary volume was increased in the simulations from 0.045 to 0.12 ml/g. According to the central volume principle the mean-transit time equals the ratio of the volume of distribution and blood flow. For the determination of the mean-transit time there should be no recirculation of tracer. In the special case of PS=0 ml/min/g (i.e., an intravascular tracer) the mean-transit time through the capillary network doubles if the capillary volume is increased two-fold. The increase in tissue impulse response amplitude calculated from simulated residue curves is by comparison only 18% when the capillary volume is increased from 0.045 to 0.08. These results agree with the observation that the maximum rate of signal enhancement during contrast agent wash-in, i.e., the maximum up-slope of the signal curve, is more sensitive to changes in flow than changes in capillary volume. Given the difficulty of determining the vascular volume, and, in particular, the capillary volume, with an extracellular tracer, we find that an estimate of the blood flow reserve based on the tissue impulse response amplitudes should be superior to estimates based on the mean-transit time.

The simulations in this study illustrate the limitations of signal curve parameters such as the peak intensity, which were used for the assessment of myocardial blood flow.[37] It can be seen from the simulated residue curves in Fig. 4 that the peak intensity after subtraction of the baseline signal rises by only 38% percent when model blood flow is increased from 1.5 to 4.0 ml/min/g. By comparison, the peak contrast enhancement changes by 25% when the capillary volume is increased from 0.04 to 0.1 ml/g. The maximum rate of signal enhancement during contrast agent wash-in is a better measure of blood flow changes.[38] A more fundamental problem with semiquantitative parameters such as the upslope or the peak intensity, is the difficulty of quantifying changes in myocardial blood flow between baseline and hyperemia, which are accompanied by changes in cardiac output. In mathematical terms this can be accomplished by deconvolution of the tissue residue curves with an arterial input function. Parameters such as the peak intensity are only suitable for the visual identification of perfusion defects in first pass images, and possibly for estimates of defect size.[39]

Both the Fermi function model and the MMID4 model used for the generation of model tissue curves allow one to deconvolve the vascular input. MMID4 is a spatially distributed, compartmental model that has been shown to be a good approximation of microvascular transport in the heart, allowing quantification of absolute blood flow.[17,25,36] It has been used to analyze the MR first pass signal versus time curves obtained with an intravascular contrast agent.[24,40] In the present study we used the extracellular contrast agent Gd-DTPA, which is not confined to the vascular space and therefore requires adjustment of 10–20 MMID4 model parameters, which may not all be identifiable from a single MR residue curve. The inclusion in the model of requirements such as local mass balance reduces the degrees of freedom and partially offsets the burden from increased complexity and realism.[17] The Fermi function model, by contrast, is a noncompartmental model with only three adjustable parameters. No information about the physiological processes underlying microvascular transport, such as the capillary permeability, can be extracted from such a model. The purpose of the simulations presented here was to establish that despite these simplifications it is possible to estimate the myocardial perfusion reserve under the experimental conditions encountered in the MR patient studies.

C. Limitations of this study

A central assumption for the analysis of the patient MR perfusion data is that the observed signal intensity in a myocardial region of interest is proportional to the tissue concentration of the Gd-DTPA contrast agent.[18,19] It remains unclear if the relaxation properties of Gd-DTPA are altered once Gd-DTPA enters the myocytes in an infarct zone. In the patient study we only included patients with no previous infarct. In practice, this uncertainty about the relaxation properties of Gd-DTPA in tissue regions with compromised cellular membranes may not be a significant limitation, as one generally wants to determine the blood flow reserve in a noninfarcted zone.

The signal modulation observed in a tissue region during contrast agent transit can extend by way of water exchange beyond the distribution space of the contrast agent. It was shown that this can lead to overestimation of the vascular volume if water exchange is neglected.[20] The effects of water exchange on the measured MR signal can be reduced with a saturation recovery sequence prepared FLASH sequence by increasing the flip angle α and keeping the repetition time (TR) as short as possible. Based on previous simulations[20] we find that the pulse sequence parameters $\alpha=18°$, TR=2.2 ms, TI=10 ms used in this study represent good parameter choices to minimize the effects of water exchange

with a T_1-weighted, spoiled gradient echo FLASH sequence. Larger flip angles drive the magnetization more rapidly into a driven equilibrium state during the FLASH image acquisition, which can cause image artifacts.

The simulations were based on the fitting of pseudodata generated by adding noise to model residue curves. The noise in the images may have a structure different from random uniform noise with zero mean. Further studies are needed to elucidate the structure of noise in MR first pass perfusion measurements. Variations in the heart rate can cause artifactual modulations of the signal versus time curves, which may be mistaken for random noise. In the present study we eliminated this source of measurement error by preceding the FLASH acquisition with a saturation recovery magnetization preparation that renders the measured signal insensitive to arrhythmias.[14,15] It is conceivable that other sources of physiological noise may modulate the observed signal versus time curves. In addition, the signal curves can be compromised by not positioning the ROI correctly, which is most likely to occur due to low tissue to blood contrast before any CA has appeared in the blood pool. The noise observed in the baseline of the signal curves may therefore not always represent the true noise from the MR measurement, and increased baseline noise would lead to an underestimate of the true C/N.

V. CONCLUSIONS

This study shows that the myocardial perfusion reserve can be determined by model-constrained deconvolution of MR signal curves and the determination of the impulse response amplitude. The assumptions of the model were tested with Monte Carlo simulations, using a multiple path, axially distributed mathematical model of the blood tissue exchange, which allowed systematic variation of the vascular volume, flow, and capillary permeability. The simulations established that the variation of the blood flow reserve estimate falls within the error range resulting from measurement noise. It was found that over a range of flows from 0.5 to 4.0 ml/min/g, the ratio of the impulse response amplitudes for hyperemic and basal flows agrees with the ratio of model blood flows, if the input function is sufficiently compact. The uncertainty in the blood flow reserve estimates grows both at low (<1.0 ml/min/g) and high ($>3-4$ ml/min/g) flows. The predictions of these simulations agree with the results of MR studies of patients without significant coronary artery lesions and microvascular dysfunction. In patients with microvascular dysfunction the perfusion reserve in the territory of the LAD correlates linearly with the CFR in the LAD, in agreement with previous PET studies.

ACKNOWLEDGMENTS

The authors would like to thank Leon Axel, M.D., Ph.D. (Department of Radiology, University of Pennsylvania) for useful discussions regarding the Fermi function model used for constrained deconvolution in this study. The late Keith Kroll, Ph.D. (National Simulation Resource, University of Washington, Seattle) constantly gave valuable suggestions and encouragement, and generously shared his profound knowledge in physiology and tracer kinetic modeling. This work was supported by grants from the RSNA Research and Education Fund (MJ-H), The Whitaker Foundation (MJ-H), and the American Heart Association (NW).

APPENDIX: MINIMIZATION OF EXCHANGE RATE DEPENDENCE WITH SATURATION-RECOVERY PREPARED FLASH IMAGING

Image contrast is primarily determined by the central Fourier k-space lines. For FLASH image acquisitions at a constant rate—e.g., one image every one to two heartbeats—the amplitude of the T_1-weighted signal after the nth phase encoding step (S_n) can be approximated with an analytical expression previously derived by Brix *et al.*:[41]

$$S_n = S_0\left[\frac{1-E}{1-a} + a^{n-1}\cdot\left(Q - \frac{1-E}{1-a}\right)\right], \tag{A1}$$

where $a = E\cdot\cos(\alpha)$ with $E = \exp(-R_1\cdot \mathrm{TR})$. S_0 is proportional to the fully relaxed magnetization M_0. The flip angle is denoted by α. Q is the quotient of the longitudinal magnetization just before the first α pulse of the FLASH acquisition, and the magnetization at thermal equilibrium, M_0. For a saturation recovery magnetization preparation the expression by Brix *et al.*[41] for Q reduces to $Q = 1-\exp(-\mathrm{TI}\cdot R_1)$ and is independent of the sequence repetition rate, or the heart rate when the sequence is ECG triggered. For this special case, Eq. (A1) can be simplified to

$$S_n = S_0\cdot\left(1-\exp\,(-R_1\cdot \mathrm{TI})\cdot a^{n-1} + (1-E)\cdot\,\frac{1-a^{n-1}}{1-a}\right). \tag{A2}$$

TI denotes here the delay time between the nonslice selective 90° pulse and the start of the FLASH acquisition. With $\alpha = 18°$, TR=2.2 ms, TI=10 ms, Eq. (A2) can be approximated by

$$S_n \approx S_0\left(\frac{\mathrm{TR}}{T_1}\cdot\,\frac{1}{1-(1-\mathrm{TR}/T_1)\cdot\cos\,\alpha}\right). \tag{A3}$$

It was previously shown that, starting from this approximation for the spoiled gradient echo signal, the effects of water exchange are minimized when[20]

$$\frac{\cos\,\alpha}{1-\cos\,\alpha}\cdot\,\frac{\mathrm{TR}}{T_1} \ll 1. \tag{A4}$$

With $\alpha = 18°$, TR=2.2 ms, TI=10 m, the left-hand side of the above inequality is on the order of 0.05 for a R_1 of $1.25\ \mathrm{s}^{-1}$ and 0.21 for $R_1 = 5.0\ \mathrm{s}^{-1}$. For 1.5 mmol/l of Gd-DTPA the T_1 relaxation rate is approximately $R_1 = 5.0\ \mathrm{s}^{-1}$. For a Gd-DTPA dosage of 0.025, as used in the patient studies, 1.5 mmol/l is approximately the average contrast agent concentration in the LV blood pool during the first pass.

[a]Please address correspondence to Michael Jerosch-Herold, Ph.D., Department of Radiology, UMHC Box 292, University of Minnesota, 420 Delaware St. SE, Minneapolis, MN 55455. Electronic mail: jeros001@tc.umn.edu

[1]K. L. Gould and K. Lipscomb, ''Effects of coronary stenosis on coronary

flow reserve and resistance,'' Am. J. Cardiol. **34**, 48–55 (1974).
[2]J. T. Cusma, E. J. Toggart, J. D. Folts, W. W. Peppler, N. J. Hangiandreou, C. Lee, and C. A. Mistretta, ''Digital subtraction angiographic imaging of coronary flow reserve,'' Circulation **75**, 461–472 (1987).
[3]R. F. Wilson, M. L. Marcus, and C. W. White, ''Prediction of the physiologic significance of coronary arterial lesions by quantitative-lesion geometry in patients with limited coronary artery disease,'' Circulation **75**, 723–732 (1987).
[4]A. L. McGinn, C. W. White, and R. F. Wilson, ''Interstudy variability of coronary flow reserve. Influence of heart rate, arterial pressure, and ventricular preload,'' Circulation **81**, 1319–1330 (1990).
[5]W. Schaper, ''The measurement of regional myocardial perfusion,'' in *The Pathophysiology of Myocardial Perfusion*, edited by W. Schaper (Elsevier/North-Holland Biomedical, Amsterdam, 1979).
[6]S. Sawada, O. Muzik, R. S. B. Beanlands, E. Wolfe, G. D. Hutchins, and M. Schwaiger, ''Interobserver and interstudy variability of myocardial blood flow and flow reserve measurements with nitrogen 13 ammonia-labeled positron emission tomography,'' J. Nucl. Cardiol. **2**, 413–422 (1995).
[7]M. E. Shelton, M. J. Senneff, P. A. Ludbrook, B. E. Sobel, and S. R. Bergmann, ''Concordance of nutritive myocardial perfusion reserve and flow velocity reserve in conductance vessels in patients with chest pain with angiographically normal coronary arteries,'' J. Nucl. Med. **34**, 717–722 (1993).
[8]N. Wilke, C. Simm, J. Zhang, J. Ellermann, X. Ya, H. Merkle, G. Path, H. Ludemann, R. J. Bache, and K. Ugurbil, ''Contrast-enhanced first pass myocardial perfusion imaging: Correlation between myocardial blood flow in dogs at rest and during hyperemia,'' Magn. Reson. Med. **29**, 485–497 (1993).
[9]J. T. Keijer, A. C. v. Rossum, M. J. v. Eenige, A. J. Karreman, M. B. Hofman, J. Valk, and C. A. Visser, ''Semiquantitation of regional myocardial blood flow in normal human subjects by first-pass magnetic resonance imaging,'' Am. Heart J. **130**, 893–901 (1995).
[10]S. E. Epstein and R. Cannon, III, ''Site of increased resistance to coronary flow in patients with angina pectoris and normal epicardial coronary arteries,'' J. Am. Coll. Cardiol. **8**, 459–461 (1986).
[11]R. F. Wilson, K. Wyche, B. V. Christensen, S. Zimmer, and D. D. Laxson, ''Effects of adenosine on human coronary arterial circulation,'' Circulation **82**, 1595–1606 (1990).
[12]R. F. Wilson, D. E. Laughlin, P. H. Ackell, W. M. Chilian, M. D. Holida, C. J. Hartley, M. L. Armstrong, M. L. Marcus, and C. W. White, ''Transluminal, subselective measurement of coronary artery blood flow velocity and vasodilator reserve in man,'' Circulation **72**, 82–92 (1985).
[13]R. F. Wilson, ''Assessment of the human coronary circulation using a Doppler catheter,'' Am. J. Cardiol. **67**, 44D–56D (1991).
[14]N. Tsekos, Y. Zhang, H. Merkle, N. Wilke, M. Jerosch-Herold, A. E. Stillman, and K. Ugurbil, ''Fast anatomical imaging of the heart and assessment of myocardial perfusion with arrythmia insensitive magnetization preparation,'' Magn. Reson. Med. **34**, 530–536 (1995).
[15]G. Laub and O. Simonetti, ''Assessment of myocardial perfusion with saturation-recovery Turbo FLASH sequences,'' ISMR, *Proceedings of the 4th Scientific Meeting of the ISMR*, New York, 1996, Vol. 1, p. 179.
[16]A. V. Clough, A. Al-Tinawi, J. H. Linehan, and C. Dawson, ''Regional transit time estimation from image residue curves,'' Ann. Biomed. Eng. **22**, 128–143 (1994).
[17]J. B. Bassingthwaighte and C. A. Goresky, ''Modeling in the analysis of solute and water exchange in the microvasculature,'' in *Handbook of Physiology—The Cardiovascular System*, edited by E. M. Renkin and C. C. Michel (American Physiology Society, Bethesda, MD, 1984).
[18]G. Strich, P. L. Hagan, K. H. Gerber, and R. A. Slutsky, ''Tissue distribution and magnetic resonance spin lattice relaxation effects of gadolinium-DTPA,'' Radiology **154**, 723–726 (1985).
[19]S. H. Koenig, M. Spiller, R. Brown, III, and G. L. Wolf, ''Relaxation of water protons in the intra- and extracellular regions of blood containing Gd(DTPA),'' Magn. Reson. Med. **3**, 791–795 (1986).
[20]K. M. Donahue, R. M. Weisskoff, D. A. Chesler, K. K. Kwong, J. Alexei, A. Bogdanov, J. B. Mandeville, and B. R. Rosen, ''Improving MR quantification of regional blood flow volume with intravascular T1 contrast agents: Accuracy, precision, and water exchange,'' Magn. Reson. Med. **36**, 858–867 (1996).
[21]I. N. Weinberg, S. C. Huang, E. J. Hoffman, L. Araujo, C. Nienaber, M. Grover-McKay, M. Dahlbom, and H. Schelbert, ''Validation of PET-acquired input functions for cardiac studies,'' J. Nucl. Med. **29**, 241–247 (1988).
[22]L. Axel, ''Tissue mean transit time from dynamic computed tomography by a simple deconvolution technique,'' Invest. Radiol. **18**, 94–99 (1983).
[23]W. H. Press, S. A. Teukolsky, W. T. Vetterling, and B. P. Flannery, *Numerical Recipes in C*: *The Art of Scientific Computing* (Cambridge University Press, Cambridge, 1992).
[24]K. Kroll, N. Wilke, M. Jerosch-Herold, Y. Wang, Y. Zhang, R. J. Bache, and J. B. Bassingthwaighte, ''Accuracy of modeling of regional myocardial flows from residue functions of an intravascular indicator,'' Am. J. Physiol. **40**, H1643–H1655 (1996).
[25]J. Kuikka, M. Levin, and J. B. Bassingthwaighte, ''Multiple tracer dilution estimates of D- and 2-deoxy-D-glucose uptake by the heart,'' Am. J. Physiol. **250**, H29–H42 (1986).
[26]G. J. Crystal, H. F. Downey, and F. A. Bashour, ''Small vessel and total coronary blood volume during intracoronary adenosine,'' Am. J. Physiol. **241**, H194–H201 (1981).
[27]H. K. Thompson, C. F. Starmer, R. E. Whalen, and H. D. McIntosh, ''Indicator transit time considered as a gamma variate,'' Circ. Res. **14**, 502–515 (1964).
[28]H. J. Weinmann, W. R. Press, and H. Gries, ''Tolerance of extracellular contrast agents for magnetic resonance imaging,'' Investig. Radiol. **25** (Suppl 1), S49–50 (1990).
[29]J. B. Bassingthwaigthe, G. R. Raymond, and J. I. S. Chan, ''Principles of tracer kinetics,'' in *Nuclear Cardiology: State of the Art and Future Directions*, edited by B. L. Zaret and G. A. Beller (Mosby-Year Book, St. Louis, 1993).
[30]H. Sakuma, L. M. Blake, T. M. Amidon, M. O'Sullivan, D. H. Szolar, A. P. Furber, M. A. Bernstein, T. K. F. Foo, and C. B. Higgins, ''Coronary Flow reserve: Noninvasive measurement in humans with breath-hold velocity encoded cine MR imaging,'' Radiology **198**, 745–750 (1996).
[31]G. D. Clarke, R. Eckels, C. Chaney, D. Smith, J. Dittrich, W. G. Hundley, N. NessAiver, H. F. Li, R. W. Parkey, and R. M. Peshock, ''Measurement of absolute epicardial coronary artery flow and flow reserve with breath-hold cine phase-contrast magnetic resonance imaging,'' Circulation **91**, 2627–2634 (1995).
[32]C. Lentner, *Heart and Circulation*, edited by C. Lentner (CIBA-GEIGY Corporation, Caldwell, NJ, 1990).
[33]W. Grossman, ''Blood flow measurement: The cardiac output,'' in *Cardiac Catheterization, Angiography and Intervention*, edited by W. Grossman and D. S. Bain (Lea & Feibiger, Philadelphia, 1991).
[34]C. Y. Tong, F. S. Prato, F. Wisenberg, T. Y. Lee, E. Carroll, D. Sandler, J. Wills, and D. Drost, ''Measurement of the extraction efficiency and distribution volume for Gd-DTPA in normal and diseased canine myocardium,'' Magn. Reson. Med. **30**, 337–346 (1993).
[35]R. B. King, J. B. Bassingthwaighte, J. R. S. Hales, and L. B. Rowell, ''Stability of heterogeneity of myocardial blood flow in normal and awake baboons,'' Circ. Res. **57**, 285–295 (1985).
[36]J. H. Caldwell, G. V. Martin, G. M. Raymond, and J. B. Bassingthwaighte, ''Regional myocardial flow and capillary permeability-surface area products are nearly proportional,'' Am. J. Physiol. **267**, H654–H666 (1994).
[37]M. F. Wendland, M. Saeed, T. Masui, N. Derugin, and C. B. Higgins, ''First pass of an MR susceptibility contrast agent through normal and ischemic heart: Gradient-recalled echo-planar imaging,'' JMRI **3**, 755–760 (1993).
[38]M. Jerosch-Herold, N. Wilke, A. E. Stillman, A. Muehler, and Y. Wang, ''Functional myocardial perfusion maps from MR first pass images,'' *Proceedings of the 3rd Annual Meeting of the Society of Magnetic Resonance* (Society of Magnetic Resonance, Nice, 1995), Vol. 1, p. 459.
[39]K. Lauerma, M. Saeed, M. F. Wendland, N. Derugin, K. K. Yu, and C. B. Higgins, ''The use of contrast-enhanced magnetic resonance imaging to define ischemic injury after reperfusion. Comparison in normal and hypertrophied hearts,'' Invest. Radiol. **29**, 527–535 (1994).
[40]N. Wilke, K. Kroll, H. Merkle, Y. Wang, Y. Ishibashi, Y. Xu, Y. Zhang, M. Jerosch-Herold, A. Muehler, A. E. Stillman, J. B. Bassingthwaighte, R. Bache, and K. Ugurbil, ''Regional myocardial blood volume and flow: First pass MR imaging with Polylysine-Gadolinium-DTPA,'' J. Magn. Reson. Imag. **5**, 227–237 (1995).
[41]G. Brix, L. R. Schad, M. Deimling, and W. J. Lorenz, ''Fast and precise T1 imaging using a TOMROP sequence,'' Magn. Reson. Med. **8**, 351–356 (1990).

Measure and Evaluate MRgRT 3D Distortion

distortioncheck

CLOUD SOFTWARE FOR EVALUATION OF IMAGE DISTORTION

SCAN

UPLOAD IMAGES

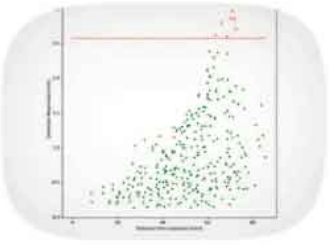

REVIEW REPORTS & TREND ANALYSIS

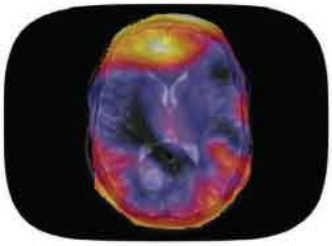

EXPORT DICOM OVERLAYS TO TPS

Large Field Grid Phantom
2152 Physical Control Points

- ✔ CIRS proprietary materials simulate distortion due to susceptibility & chemical shifts typical to clinical patient scans
- ✔ Density of physical control points optimized to bring interpolation close to linearity
- ✔ Cloud based solution frees user of operating system and hardware constraints
- ✔ Quickly & automatically analyze complete MR data sets
- ✔ Online deployment facilitates collaboration, easy review and portability of results

Inter-cranial Grid Phantom
335 Physical Control Points

CIRS
Tissue Simulation & Phantom Technology

cirsinc.com
900 Asbury Ave., Norfolk, VA 23513, USA • (800) 617-1177